and it is believed that they would also be greater for wider continuous structures of equal length. Savings are realized at the expense of significant increases in design effort. The alternative to expenditure of this effort for heavily skewed boxes may be very unrepresentative designs. Automation of program input, output interpretation, and development of expertise on the part of designers would be essential to realization of appreciable savings.

ACKNOWLEDGMENT

Design, construction, and testing of the skew box-girder model were performed in conjunction with a research project entitled, Structural Behavior of a Skew, Reinforced Concrete Box-Girder Bridge Model, which was sponsored jointly by the Federal Highway Administration (FHWA) and Caltrans.

The opinions, findings, and conclusions expressed in this paper are mine and do not necessarily reflect the official views or policies of Caltrans or FHWA. This paper does not constitute a standard, specification, or regulation.

REFERENCES

1. R.E. Davis. Structural Behavior of a Skew, Reinforced Concrete Box Girder Bridge Model: Volume 1, Design. Office of Structures Design, California Department of Transportation, Sacramento, Rept. FHWA-CA-50-4187-78-01, Jan. 1978.
2. R.E. Davis, J.J. Kozak, and C.F. Scheffey. Structural Behavior of a Box Girder Bridge. HRB, Highway Research Record 76, 1965, pp. 32-82.
3. R.E. Davis, J.J. Kozak, and C.F. Scheffey. Structural Behavior of a Box Girder Bridge, and Appendices. Bridge Department, California Division of Highways, Sacramento, Rept. SSR 2-65, 1965.
4. R.E. Davis, C.F. Scheffey, G.A. Castleton, and E.E. Evans. Box Girder Model Studies. Bridge Department, California Division of Highways, Sacramento, Rept. R&D 4-70, 1970.
5. R.E. Davis, C.F. Scheffey, G.A. Castleton, and E.E. Evans. Model and Prototype Studies of a Box Girder Bridge. Journal of the Structural Division, ASCE, Jan. 1972.
6. K.J. Willam and A.C. Scordelis. Computer Program for Cellular Structures of Arbitrary Plan Geometry. Univ. of California, Berkeley, Structural Engineering and Structural Mechanics Rept. UC SESM 70-10, Sept. 1970.

Publication of this paper sponsored by Committee on Concrete Bridges.

Response of 45° Skew, Reinforced Concrete Box-Girder Bridge Model to AASHTO Trucks and Overload Construction Vehicles

ALEX C. SCORDELIS, JACK G. BOUWKAMP, S. TANVIR WASTI, AND FRIEDER SEIBLE

A detailed study of the structural response of a 45° skew, two-span, four-cell, reinforced concrete box-girder bridge model under different types of vehicle loading is presented. The model, which was a 1:2.82 scale replica of a typical California highway prototype bridge, was 72 ft (21 m) long by 12 ft (3.7 m) wide and was supported by 45° skew end abutments and a 45° skew center bent supported by a single column. The vehicle loadings used consisted of scale models of standard American Association of State Highway and Transportation Officials HS 20-44 trucks and overload construction vehicles (class 2). In addition, influence lines for reactions and deflections were obtained by positioning a forklift truck at selected points on the bridge deck. The experimental response of the bridge model in the form of reactions, deflections, moments, and steel and concrete strains is compared with the theoretical response values obtained from a finite-element computer program CELL. The influence of skewness on the major design quantities is also assessed.

Multicell reinforced concrete box-girder bridges are widely used in the California highway system. The growing number of complex intersections, the lack of space in crowded urban areas, and the demand for road layouts without abrupt changes in direction frequently necessitate the use of bridges with skew, curved, or arbitrary plan geometry. Most design calculations for live load distribution in straight, skew, and curved box-girder bridges are based on the same empirical formula in which the effects of skewness or curvature are generally ignored.

The 1977 American Association of State Highway and Transportation Officials (AASHTO) specifications (1) specify a design method wherein a box-girder bridge is divided up into a number of interior girders plus two exterior girders. Each of these girders is designed as a separate member by applying to it a certain fraction of a single longitudinal line of wheel loads from a standard AASHTO HS 20-44 truck. The fraction is $N_{WL} = S/7$, in which S is the web spacing.

California uses a design procedure in which the whole bridge width is considered as a single unit and the distribution factor for the whole width unit is given by N_{WL} (total) = deck width in feet/7. The total moment at any section is assumed to be uniformly distributed across the width of the bridge.

In current practice for a skew bridge, design live load moments are determined for either of the above empirical wheel loadings by analyzing a straight bridge that has the same span but without any skew. Empirical rules, approximations, and engineering judgment are then used to account for skewness in determining longitudinal reinforcement cutoff points and some increase in web reinforcement for shear in the obtuse corners of the bridge.

In fact, the presence of skew generally reduces the total midspan moments in box-girder bridges because of the distribution of the reactions along the end abutments. The reduced moment for a simple span, 45° skew, four-cell box-girder bridge is shown in Figure 1 for a uniformly distributed surface load calculated with the finite-element computer program CELL (2) and compared with the generally used solu-

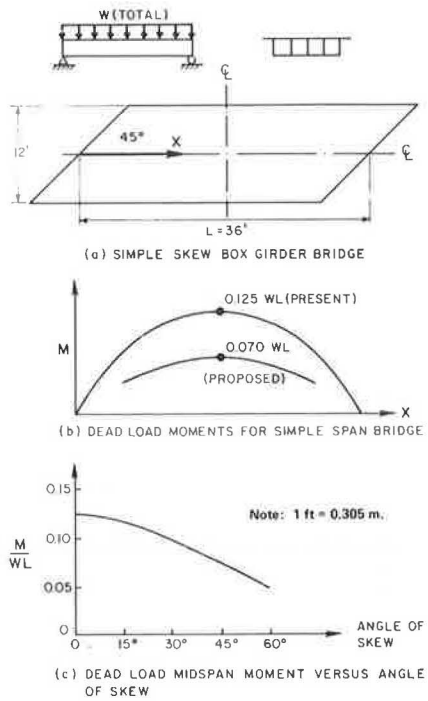

Figure 1. Reduction of total dead load moment at section due to skewness.

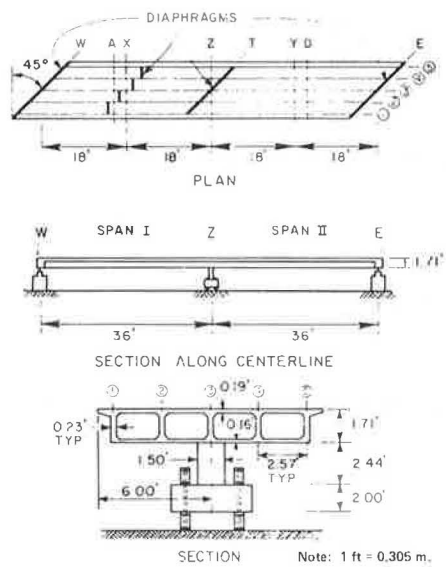

Figure 2. Overall dimensions of bridge model.

tion for a similar straight bridge model with the same span. The variation of the total midspan moment with the change in the angle of skew is also shown in Figure 1. Comartin and Scordelis (3) put forward a simplified design method for the design of simply supported skew box girders and have recommended the use of the computer program CELL for the design of continuous skew box-girder bridges. Godden and Aslam (4) verified the theoretical results from CELL by testing small-scale 1:29 elastic aluminum models of skew box-girder bridges. Also, a detailed study of 51 mathematical models of skew reinforced concrete box-girder bridges by using CELL has been reported by Wallace (5).

A continuous research program on box-girder bridges, which is directed toward improved design methods, has been conducted at the University of California, Berkeley, in which analytical and experimental studies have been successively conducted on the structural behavior of box-girder bridges that are straight, curved, skew, or of arbitrary plan geometry (6-19, and paper by Davis in this Record). As part of this investigation, a large number of computer programs have been developed for the analysis of these bridges by using folded-plate, finite-strip, finite-element, or finite-segment methods. A summary of these programs (with examples) can be found elsewhere (6). In addition, a number of the analytical and experimental investigations are summarized by Scordelis (7).

The most recent extensive investigation was made on the behavior of a 45° skew, two-span, four-cell, reinforced concrete box-girder bridge model (16). In this paper, the bridge behavior under standard AASHTO truck loads, construction-vehicle overloads, and moving forklift loads is studied in detail, and the influence of skewness on the major design quantities is assessed. Other aspects of the investigation, such as the structural response of the bridge model to point loads at working stress and overload stress levels (17), the behavior under conditioning overloads and ultimate failure loads (18), and the time-dependent behavior under sustained dead load (19), have been reported on elsewhere.

CONSTRUCTION OF BRIDGE MODEL AND EXPERIMENTAL PROGRAM

The overall dimensions of the 45° skew, two-span, four-cell, reinforced concrete bridge model as well as the designation of longitudinal girder lines and transverse sections are shown in Figure 2. The bridge was supported by 45° skew end abutments and a 45° skew center bent supported by a single circular column. The model was a 1:2.82 scale replica of a typical California two-lane box-girder bridge. The chosen scale guaranteed true representation of material behavior and was determined from the size of the standard reinforcing bars [60 ksi (414 MPa) yield] used in the prototype and model. A No. 11 main longitudinal bar in the prototype was exactly simulated by a No. 4 bar in the model.

The bridge model was designed by the Structural Research Unit, Office of Structures, California Department of Transportation (Caltrans), and was constructed by an outside contractor in the Structural Engineering Laboratory, Davis Hall, University of California, Berkeley. The design of the skew model, which is described in detail in Davis (see paper in this Record), was made with the aid of the CELL program (2) and resulted in the use of No. 4 reinforcement that was, by total volume, only about 81 percent of that that would be used in a similar straight bridge on orthogonal supports that had the same spans.

A brief summary of the construction of the bridge model and the test setup is given in Figure 3. Figures 3a, b, c, d, and g depict various stages in the construction of the bridge model, which was done in the same manner as the contruction of a prototype in the field. Figure 3e shows the additional dead load in the form of concrete blocks, which was necessary to simulate the proper prototype dead load behavior. Figure 3f illustrates the two midspan loading frames used for the application of point loads, AASHTO truck loads, and failure loads, respectively. Figure 3h shows the bridge model during the final load test to failure.

The instrumentation of the model was designed to measure loads, reactions, deflections, and strains. Load cells were used to measure individual end reactions under each girder, column reactions at the center bent, and loads applied by means of hydraulic jacks at midspan sections X and Y. Deflections were

measured at 32 points by linear potentiometers as well as by mirror scales along the exterior girders of the bridge model. Steel strains were monitored by 128 waterproofed, weldable strain gages and concrete strains by 86 concrete strain meters. A low-speed scanner unit with 8K storage, magnetic tape recorder, digital voltmeter, teletype, and terminal boxes controlled and recorded the measurements.

The experimental program consisted of the following parts: (a) dead load, (b) working stress loads, (c) overloads, and (d) failure loading. The application of AASHTO truck loads, construction-vehicle overloads, and moving forklift truck loads was conducted as part of the working stress load stage after the bridge model had been subjected to conditioning loads that produced nominal tensile stresses of 30 ksi (207 MPa) in the reinforcing steel. In order to allow the positioning of the truck models on the bridge deck, the concrete blocks that represented part of the prototype dead load shown in Figure 3e had to be removed.

The AASHTO truck models, one of the construction vehicles, and the forklift truck used for the loading of the skew bridge model are shown in Figures 4a, b, and c, respectively.

Figure 3. Sequence of construction, overall test setup, and loading to failure of skew bridge model.

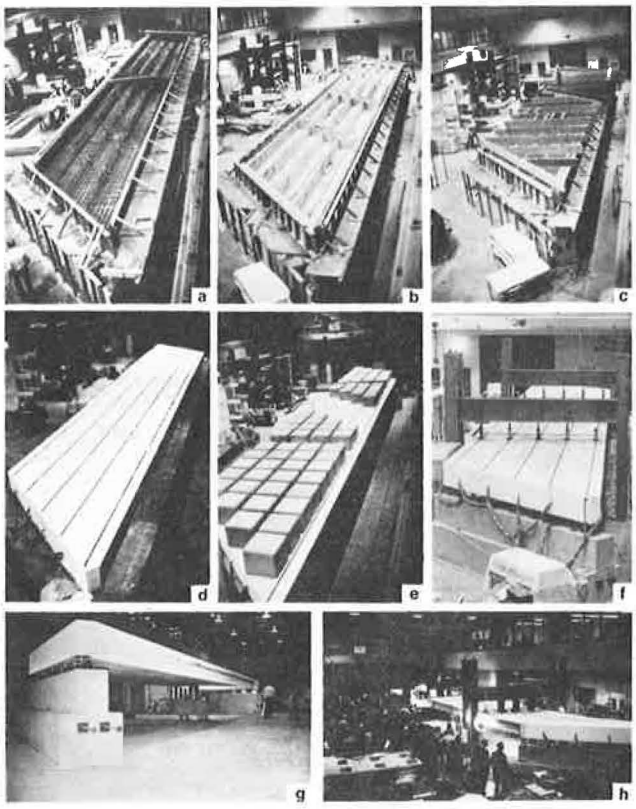

Figure 4. AASHTO trucks, construction vehicles, and moving forklift truck on bridge deck.

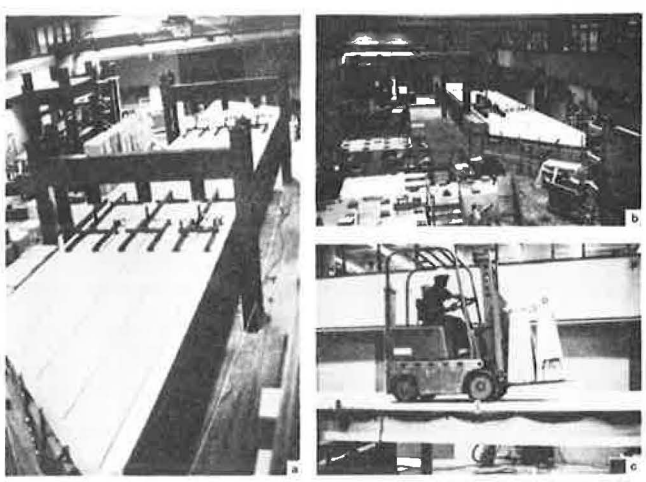

THEORETICAL ANALYSIS

For comparison with experimental data, a theoretical analysis was conducted by using the computer program CELL (2), which is a general finite-element program for the linear elastic analysis of cellular bridge structures in which the structure is assumed to be an uncracked homogeneous concrete assemblage of plane plate elements that represent the top and bottom flanges and the vertical webs. Both membrane and plate-bending action are accounted for in the elements comprising the structure. Convergences and accuracy of solutions were assured by comparing different mesh sizes and by statics checks of external and internal forces at various sections in the bridge model.

As in the AASHTO specifications, each truck was modeled by six vertical concentrated loads that were appropriately scaled down to simulate the prototype loads on the model (Figures 4a and b). The moving forklift truck was modeled in the theoretical analysis by four vertical point loads (Figure 4c).

The results from the theoretical analysis by using CELL were in the form of reactions, deflections, and internal forces. The internal forces were directly converted by a postprocessor program to individual girder and total sections moments at various transverse sections of the bridge model for direct comparison with similarly reduced experimental data.

AASHTO TRUCK AND CONSTRUCTION-VEHICLE LOADING

The model was loaded by scaled-down versions of the standard AASHTO HS 20-44 (MS 18) truck [truck load = 72 kips (320 kN)] and a proposed overload class 2 construction vehicle [total load = 320 kips (1470 kN)]. All linear dimensions were reduced by the scale factor 1:2.82, and similitude required that the loads be reduced by a factor of 1:8 to produce the same stress in the model as in the prototype. Thus, for the model the total load for each truck was 9.0 kips (40.0 kN) and for each construction vehicle 41.25 kips (183.5 kN).

The positions and directions of the truck and construction-vehicle loads on the bridge are shown in Figure 5 (also Figure 4). A total of 11 combinations of two-lane truck loadings, 3 combinations of three-lane truck loadings, and 8 combinations of construction-vehicle loadings were used.

Reactions

A summary of experimental and theoretical reactions is given in Table 1 for selected cases of vehicle loadings. The total west end and east end reactions shown are the statically equivalent bridge centerline reactions obtained from individual reactions under each girder for both experiment and theory.

Excellent agreement exists for the vertical end reactions R_W and R_E, while the vertical center footing reaction R_F is slightly higher in the experimental than in the theoretical analysis. The

moment and torque reactions (M and T) show generally good agreement between experiment and theory except for a few load cases.

The influence of skewness of the end abutments can readily be seen from the direction and magnitude of the total end moments M_W and M_E, which for most load cases act in a sense so as to reduce the midspan moments produced by the vehicle loads.

Figure 5. Positions and directions of truck and construction-vehicle loadings on bridge deck.

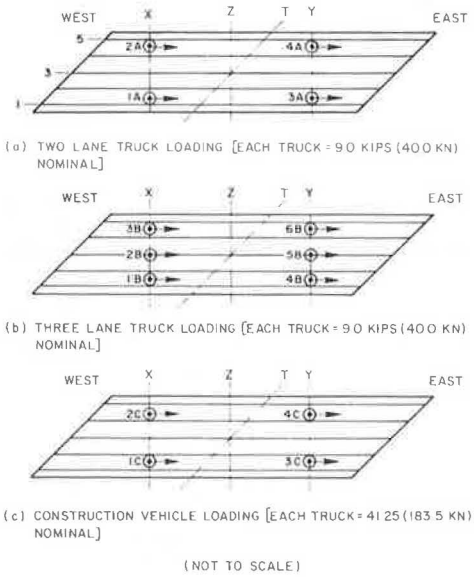

Deflections

Experimental deflections are shown in Figure 6a for vehicle loadings producing maximum deflection at transverse sections X and Y in the diaphragmed and undiaphragmed span, respectively. Theoretical values are not shown, since the analysis, which is based on an uncracked structure, does not give displacement values that can be directly compared with the experimental results obtained from the cracked reinforced concrete model. However, it should be noted that with a magnification factor of about 1.5-2.0 applied to the theoretical deflections from CELL (3), the overall shape of the deflected experimental model can be very closely approximated for all load cases in the working stress range.

For the two- and three-lane truck loads shown in Figure 5, the loading is relatively uniform across the width of the bridge, which results in an almost uniform distribution of deflections that have slightly higher deflections toward the acute side of the span. For the construction vehicle, only one lane is loaded on the acute side of the span, which results in substantially larger deflections at the loaded position. By comparing results at sections X and Y, these loadings also demonstrate the effect of the transverse midspan diaphragm. For construction-vehicle loads at position 2C and 4C (Figure 5) in the diaphragmed and undiaphragmed spans 1 and 2, respectively (Figure 1), it can be seen in Figure 6a that the transverse distribution of deflections is slightly more uniform in the diaphragmed span.

The maximum deflections for the two-lane truck, three-lane truck, and construction-vehicle loadings

Table 1. Comparison of theoretical and experimental reactions under truck and construction-vehicle loads.

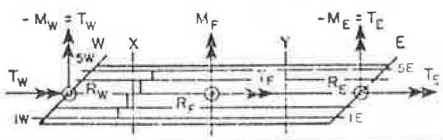

Load Case	Solution	Reactions: West End R_W (kips)	West End M_W (kip-ft)	West End T_W (kip-ft)	Center Footing R_F (kips)	Center Footing M_F (kip-ft)	Center Footing T_F (kip-ft)	East End R_E (kips)	East End M_E (kip-ft)	East End T_E (kip-ft)	Total R (kips)	Load (kips): Section X (P_X)	Section Y (P_Y)	Total (P)
Two-Lane Truck Loading														
4A	T	-0.5	-9	9	6.5	-10	15	3.1	-11	11	9.0	-9.0	0.0	-9.0
	E	-0.6	-7	7	7.0	-9	15	3.1	-14	14	9.6	-9.0	0.0	-9.0
3A+4A	T	-1.2	-4	4	11.8	-16	12	7.5	17	-17	18.0	-18.0	0.0	-18.0
	E	-1.4	-1	1	12.0	-17	11	7.3	12	-12	17.8	-18.0	0.0	-18.0
2A+4A	T	4.2	-37	37	11.5	-4	17	2.4	-15	15	18.0	-9.0	-9.0	-18.0
	E	4.0	-34	34	12.7	-2	20	2.5	-20	20	19.2	-9.0	-9.0	-18.0
1A+2A +3A+4A	T	6.7	-22	22	23.0	0	0	6.3	21	-21	36.0	-18.0	-18.0	-36.0
	E	6.5	-15	15	23.9	4	-1	6.2	16	-16	36.6	-17.8	-18.2	-36.0
Three-Lane Truck Loading														
4B+5B+6B	T	-1.8	-26	26	17.6	-24	18	11.2	7	-7	27.0	0.0	-27.0	-27.0
	E	-2.0	-1	1	18.1	-27	17	11.0	21	-21	27.1	0.0	-27.0	-27.0
1B+2B+3B +4B+5B+6B	T	10.1	-32	32	34.5	0	0	9.4	31	-31	54.0	-27.0	-27.0	-54.0
	E	9.4	-22	22	35.1	5	-1	9.1	22	-22	53.6	-27.1	-26.9	-54.0
Construction-Vehicle Loading														
4C	T	-2.1	-35	35	28.5	-40	58	14.9	-39	39	41.2	0.0	-41.3	-41.3
	E	-2.5	-27	27	30.5	-52	70	15.2	-52	52	43.2	0.0	-41.3	-41.3
2C+4C	T	18.9	-147	147	51.6	-14	64	12.0	-55	55	82.5	-41.3	-41.2	-82.5
	E	18.4	-138	138	56.5	-20	86	12.3	-69	69	87.1	-41.3	-41.2	-82.5

Notes: T = theoretical and E = experimental.
1 kip = 4.448 kN, 1 kip-ft = 1.356 kN-m.

Figure 6. Transverse distribution of deflections (inches) and strains (μ-strains) at midspan.

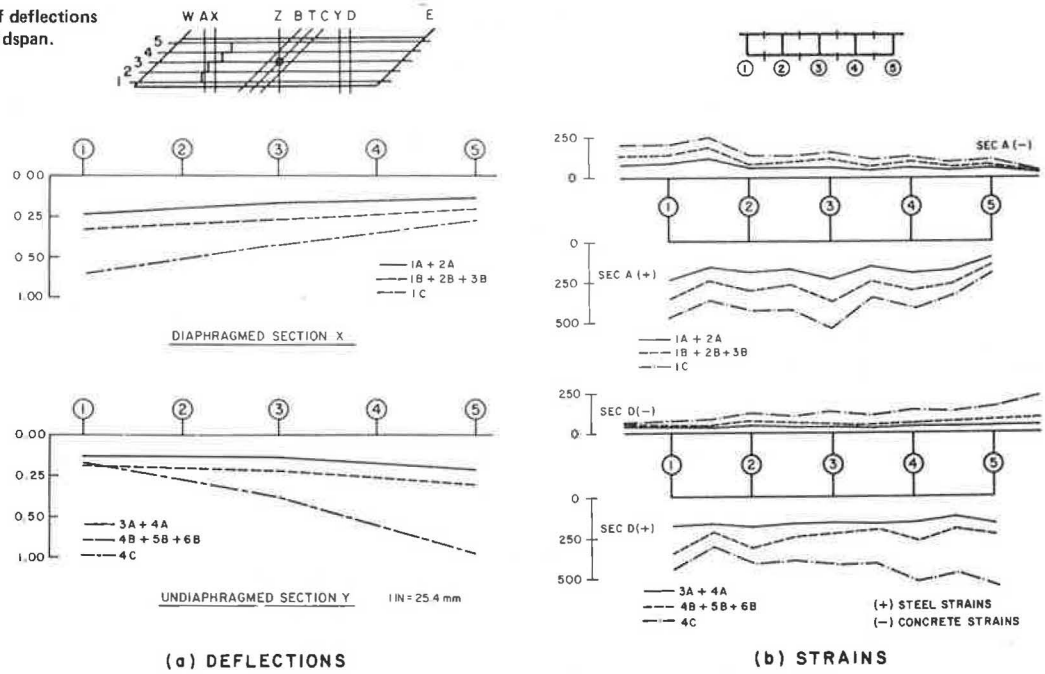

were 0.22, 0.33, and 0.74 in (5.6, 8.4, and 18.8 mm), respectively. The corresponding deflection to span ratios were 1/1960, 1/1300, and 1/580, and these would be the same in a full-scale prototype structure because of similitude.

Strains and Maximum Stresses

The transverse distribution of experimental longitudinal strains at midspan sections A and D for truck and construction-vehicle loadings producing maximum effects are shown in Figure 6b. Similar to the transverse distribution of displacements in Figure 6a, the two- and three-lane truck loadings, which are uniform across the width of the bridge, show strain distributions that are also quite uniform. For the heavy concentrated load of a construction vehicle on the acute side of the diaphragmed span 1C, only small changes in the general shape of the transverse strain distribution are noticeable at section A, while at section D for a load in the undiaphragmed span 4C, a shift of the longitudinal strains toward the loaded (acute side) of the span can be noticed.

Multiplying the maximum strain values from Figure 6b by the modulus of elasticity of the reinforcing steel and adding the nominal average dead load steel stress for sections A and D of 12 000 psi (83 MPa), it can be seen that the total maximum steel stress for the two- and three-lane truck loadings of 18 450 and 22 100 psi (127 and 152 MPa), respectively, is below the allowable value of 24 000 psi (165 MPa). For the construction-vehicle loading, a maximum calculated total steel stress of about 27 000 psi (186 MPa) occurs.

Live load concrete stresses calculated from compressive strains are quite small and would be well within the allowable stresses when added to the nominal dead load stresses.

Total Moments and Individual Girder Moments

Tables 2, 3, and 4 summarize the girder moments and their transverse distribution for a variety of vehicle load combinations. (For truck locations, see Figure 5.)

The maximum moments in the bridge model get progressively larger as one proceeds from the single truck load to two-lane truck, three-lane truck, and finally the construction-vehicle loading. By comparing the total experimental and theoretical section moments, fairly good agreement can be found in the diaphragmed span (section A), while in the undiaphragmed span (section D) the experimental moment was found to be consistently higher than the theoretical moment. Looking at individual girder moments, it can be seen that, at section A, consistently a much larger moment is carried in girder 1 experimentally than that predicted by theory. Here the close proximity of the staggered midspan diaphragm (Figure 1) to the instrumented section A may have caused this discrepancy. The percentage distribution of total midspan moments to individual girders for critical vehicle loads in Table 4 shows that the experimental distribution is virtually the same for two-lane truck, three-lane truck, and construction-vehicle loading in the diaphragmed span, while in the undiaphragmed span at section D the construction-vehicle loading clearly shows a shift in the transverse distribution of the midspan moment to the acute side of the span. By comparing these percentage values with optimum ones obtained for a uniform stress distribution across the bridge, the two- and three-lane truck loadings in section D show good agreement, while the construction-vehicle loading deviates significantly. At section A, again, the high experimental contribution of girder 1 can be noted causing a stronger deviation from the uniform stress distribution.

Effect of Skewness: Comparison with Straight and Curved Box-Girder Bridge Models

To show the effect of skewness on reactions, deflections, strains, and moments in a continuous multicell box-girder bridge under vehicle loading, the following three cases are considered:

1. A fairly uniform vehicle loading across one span (4B+5B+6B),
2. A concentrated vehicle load on the obtuse side of a span (3C), and

Table 2. Section A experimental and theoretical girder moments under critical truck and construction-vehicle loads (moments about gross section neutral axis).

	Single Truck Loading (kip-ft)				Two-Lane Truck Loading (kip-ft)						Three-Lane Truck Loading (kip-ft)				Construction-Vehicle Loading (kip-ft)							
	1A		2A		1A+2A		1A+3A		1A+2A+ 3A+4A		1B+2B+3B		1B+2B+3B+ 4B+5B+6B		1C		2C		1C+3C		1C+4C	
Girder	E	T	E	T	E	T	E	T	E	T	E	T	E	T	E	T	E	T	E	T	E	T
1	16	10	7	5	23	15	14	9	18	12	37	24	27	18	53	31	32	21	44	26	35	20
2	15	16	6	7	21	21	13	12	17	16	33	32	26	24	48	46	29	29	41	40	33	31
3	12	14	7	7	20	21	11	12	16	16	33	32	26	24	48	47	29	26	41	41	34	32
4	10	11	9	10	19	22	8	10	15	16	29	32	22	24	41	44	29	30	33	37	27	29
5	5	8	7	9	12	16	5	7	9	13	18	23	13	17	24	31	20	23	19	26	15	20
Σ	58	59	36	38	95	95	51	50	75	73	150	143	114	107	214	199	139	129	178	170	144	132

Notes: E = experimental and T = theoretical.
1 kip-ft = 1.356 kN-m.

Table 3. Section D experimental and theoretical girder moments under critical truck and construction-vehicle loads (moments about gross section neutral axis).

	Single Truck Loading (kip-ft)				Two-Lane Truck Loading (kip-ft)						Three-Lane Truck Loading (kip-ft)				Construction-Vehicle Loading (kip-ft)							
	4A		3A		4A+3A		4A+2A		1A+2A+ 3A+4A		4B+5B+6B		1B+2B+3B+ 4B+5B+6B		4C		3C		2C+4C		2C+3C	
Girder	E	T	E	T	E	T	E	T	E	T	E	T	E	T	E	T	E	T	E	T	E	T
1	8	7	10	8	18	15	6	6	14	11	26	22	20	16	34	29	43	33	28	24	37	27
2	11	10	11	9	21	20	10	9	16	15	33	30	25	23	48	42	48	38	41	35	42	31
3	11	12	7	8	18	20	10	10	14	14	29	30	22	23	49	49	32	33	43	42	26	27
4	13	14	7	6	19	20	12	13	13	15	28	31	20	23	56	54	27	27	50	48	22	21
5	13	11	5	4	19	16	12	10	14	12	27	23	21	17	57	44	25	18	53	39	19	14
Σ	56	54	40	35	95	91	50	48	71	67	143	136	108	102	244	218	175	149	215	188	146	120

Notes: E = experimental and T = theoretical.
1 kip-ft = 1.356 kN-m.

Table 4. Experimental percentage distribution of total moment at sections A and D for critical truck and construction-vehicle loadings.

	Section A Girders					Section D Girders				
Item	1	2	3	4	5	1	2	3	4	5
Uniform stress distribution	17	22	22	22	17	17	22	22	22	17
Two-lane truck										
1A+2A	24	22	21	20	13					
3A+4A						19	22	19	20	20
Three-lane truck										
1B+2B+3B	25	22	22	19	12					
4B+5B+6B						19	23	20	20	19
Construction vehicle										
1C	25	22	22	19	12					
4C						14	20	20	23	23

3. A concentrated vehicle load on the acute side of a span (4C).

The above three loading cases are compared in Table 5 with corresponding loading cases on similar straight and curved bridge models (10,12) tested previously.

A comparison of the vertical reactions R_W, R_F, and R_E in Table 5 (see key above Table 1) shows excellent agreement between the three bridge types for all load cases except 3C where, in the case of the skew bridge, the construction vehicle is located on the obtuse side of the span and more load is transferred directly into the end abutment and less into the center footing than for the comparable straight and curved bridge cases. The end moments M_W and M_E, which are only present for the skew bridge, clearly show the characteristics of skew bridge behavior. Considering only the loaded undiaphragmed span 2 (Figure 1) and the end moment in this span (M_E), it is found that for the case where the loads are uniformly distributed across the width (4B+5B+6B) and for the case where the span is loaded on the obtuse side (3C), the end moment M_E is positive, which means the midspan moment due to the vehicle loading is effectively reduced by this end moment. However, in the case where the acute side of the span is loaded (4C), the end moment M_E is negative and thus unfavorably increases the midspan moment due to this midspan vehicle load.

The total midspan moments at section D at the bottom of Table 5 clearly show this influence of skewness. Although straight and curved bridges show good agreement for all three load cases, the skew bridge features a lower total midspan moment when the load is applied on the obtuse side of the span and a higher total midspan moment when the load is applied on the acute side of the span.

The same phenomenon can be seen from the vertical deflections across midspan section Y. Although the skew bridge deflections are much smaller for the load on the obtuse side of the skew span (3C) than for comparable straight and curved bridge cases, significantly higher deformations are encountered in the skew bridge when the vehicle is placed on the acute side of the span.

A final comparison of results for the straight, curved, and skew bridge model is made in Table 6 for maximum live load experimental strains and stresses under truck and construction-vehicle loadings. Strains shown are the maximum values recorded at any point in the bridge model under the loadings shown. From Table 6 it can be seen that the concrete strains are very low for all three bridge types. The order of magnitude for concrete and steel strains and stresses is about the same for straight, curved, and skew bridge models.

Table 5. Comparison between straight, curved, and skew box-girder bridge models.

Item	Three-Lane Truck, 4B+5B+6B			Construction Vehicle, 3C			Construction Vehicle, 4C		
	Straight	Curved	Skew	Straight	Curved	Skew	Straight	Curved	Skew
Reactions									
R_W (kips)	-2.0	-2.1	-2.0	-3.0	-2.5	-3.2	-3.0	-3.5	-2.5
M_W (kip-ft)	0.0	0.0	1.0	0.0	0.0	18.4	0.0	0.0	-26.3
R_F (kips)	18.8	18.8	18.1	28.6	27.7	24.5	28.6	28.9	30.5
R_E (kips)	10.5	9.9	11.0	16.2	16.4	20.5	16.2	15.9	15.2
M_E kip-ft)	0.0	0.0	20.5	0.0	0.0	112.5	0.0	0.0	-51.6
Deflections (in)									
1Y	0.25	0.27	0.19	0.49	0.56	0.37	0.25	0.28	0.20
3Y	0.23	0.28	0.22	0.35	0.39	0.25	0.35	0.43	0.38
5Y	0.23	0.31	0.30	0.25	0.30	0.24	0.49	0.64	0.74
Moments, section D (kip-ft)									
1	25	19	26	30	41	43	29	21	34
2	30	32	33	49	57	48	39	39	48
3	33	30	29	44	40	32	44	42	49
4	37	34	28	39	36	27	49	52	56
5	21	24	27	29	25	25	30	36	58
Total	146	139	143	191	199	175	191	190	245

Note: 1 kip = 4.448 kN, 1 kip-ft = 1.356 kN-m, 1 in = 25.4 mm.

Table 6. Comparison of maximum live load experimental strains and stresses for straight, curved, and skew bridge models under truck and construction-vehicle loads.

Item	Concrete Sections				Steel Sections			
	A	B	C	D	A	B	C	D
Experimental strains (μ in/in)								
Two-lane truck								
Straight	59	81	83	65	276	128	133	229
Curved	110	67	70	83	221	123	125	197
Skew	116	103	88	67	233	124	123	174
Three-lane truck								
Straight	72	123	119	100	334	202	201	369
Curved	138	99	110	127	306	195	200	290
Skew	175	145	129	98	365	185	183	340
Construction vehicle								
Straight	135	176	177	115	586	352	324	448
Curved	191	154	155	178	565	303	324	450
Skew	249	175	225	230	527	249	338	519
Experimental stresses (psi)								
Two-lane truck								
Straight	207	235	241	249	8 030	3 710	3860	6 690
Curved	297	178	186	254	6 080	3 380	3440	3 420
Skew	348	309	264	201	6 450	3 440	3410	4 820
Three-lane truck								
Straight	276	351	346	383	9 980	5 850	5830	10 700
Curved	373	263	292	387	8 420	5 360	5500	7 980
Skew	525	435	387	294	10 100	5 130	5070	9 420
Construction vehicle								
Straight	516	510	514	440	17 000	10 200	9380	13 000
Curved	516	408	411	543	15 500	8 330	8910	12 400
Skew	747	525	675	690	14 600	6 900	9360	14 400

Note: 1 psi = 0.006 895 MPa.

MOVING FORKLIFT TRUCK LOADINGS

For highway bridges, the most critical live loads are moving concentrated loads (such as heavy overload construction vehicles) traveling across the bridge. Therefore, part of this investigation of vehicle loadings on a skew, continuous box-girder bridge consisted of a moving forklift truck positioned at 50 selected points on the bridge deck in order to obtain general shapes of influence lines for different important design quantities. Selected influence lines for the total vertical and moment reactions at the west end abutment, as well as vertical deflections at the exterior girders of midspan section Y, are given in Figures 7 and 8.

From the general shape of these influence lines, the overall behavior of the bridge model under moving loads can be deduced, but they should not be used to obtain numerical design quantities. Scaling factors obtained from extreme or midspan values were used on the theoretical data (shown in Figures 7 and 8) to account for stiffness deterioration due to cracking in the reinforced concrete model in order to allow a comparison of the general shape of theoretical and experimental influence lines. Scaling factors and reference locations are also indicated in Figures 7 and 8.

Influence Lines for Reactions

Influence lines for the west end reactions are depicted in Figures 7a and b. For the vertical reaction, a remarkable agreement between experimental and theoretical values can be observed. It also should be noted that the scaling factors involved are very close to unity.

Influence lines for the west end moment show close agreement for the north and center pass between experiment and theory. The south pass features larger discrepancies in both general shape and scaling factor. The influence lines for the west end moment clearly show the influence of skewness of the bridge model, since the end moment directly influences the important midspan design moment. In

Figure 7. Shapes of influence lines for west end reactions.

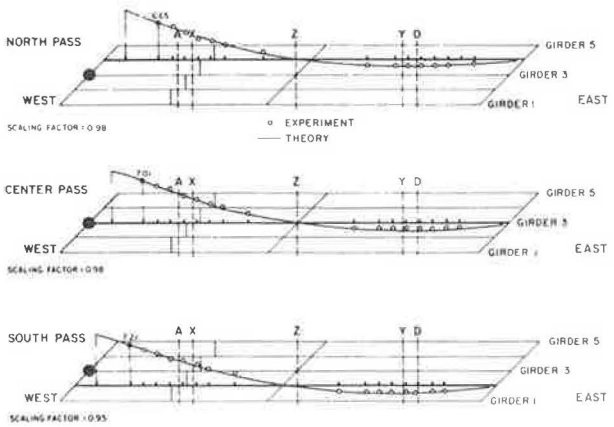

(a) TOTAL VERTICAL WEST END REACTION

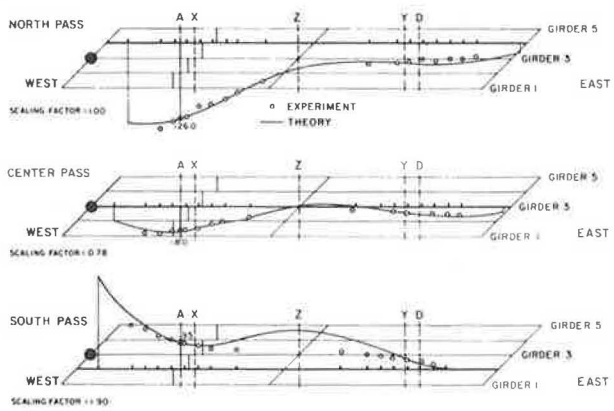

(b) TOTAL WEST END MOMENT

Figure 8. Shapes of influence lines for vertical midspan deflections.

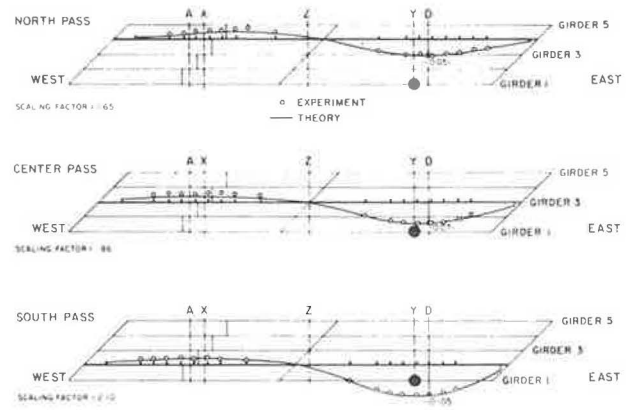

(a) DEFLECTION AT LOCATION 1Y

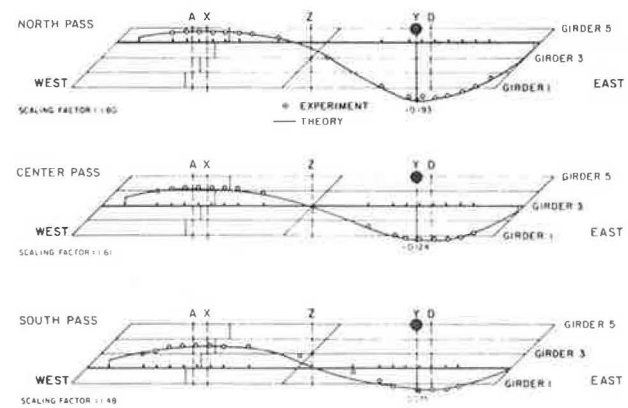

(b) DEFLECTION AT LOCATION 5Y

Figure 7b, an end moment value below the reference axis indicates a beneficial reduction in the total midspan moment, while an end moment value above the reference axis shows an unfavorable increase in the midspan moment. Thus, from Figure 7b it can be clearly seen that as long as concentrated loads move along the center of the bridge or on the obtuse side of the span, the skewness of the bridge model has a beneficial effect on the design midspan moment, while the midspan moment for a concentrated load moving along the acute side of a span will be unfavorably influenced by the skewness of the bridge.

Influence Lines for Midspan Deflections

Influence lines for midspan deflections at 1Y and 5Y in the undiaphragmed span are shown in Figures 8a and b. Again, remarkable agreement can be noticed in the general shape of the experimental and theoretical influence lines. A magnification factor between 1.5 and 2.0 is necessary to account for stiffness deterioration in the bridge model due to cracking of the concrete.

The influence of skew is seen again when comparing displacement values at the obtuse and acute side of the span in Figures 8a and b, respectively. Although the displacements on the acute side of the span are generally larger for all load positions than corresponding displacements on the obtuse side of the span, a big increase in maximum midspan displacements can be observed for loads shifting transversely across the bridge from the obtuse side to the acute side of the span.

SUMMARY AND CONCLUSIONS

The box-girder bridge model tested in this investigation clearly showed different behavior under various types of vehicle loadings than similar straight and curved bridge models, which can be attributed to the presence of skew end abutments and the skew center diaphragm. The influence of skewness depends largely on the type of loading and, more specifically, on the location of load application on the skew bridge deck.

The following conclusions can be drawn from the present investigation:

1. In addition to the vertical end reaction, a skew bridge also features an end moment that acts along an axis perpendicular to the bridge axis, which directly influences the design total midspan moments. Concentrated loads on the acute side of a span result in an end moment reaction that increases the midspan moment, while all other load positions and distributed loads across the span produce an end moment that reduces the midspan moment favorably.
2. The largest deflections under any vehicle load occurred at midspan at the acute side of the bridge loaded with a single overload class 2 con-

struction vehicle at the same location. The maximum deflection observed for this load case gives a deflection-to-span ratio of 1/580, which is still quite small but substantially larger than the comparable ratio for the similar straight bridge model of 1/870. However, the same load on the obtuse side of the span of the skew continuous bridge produced only a deflection-to-span ratio of 1/1170.

3. The transverse distribution of maximum moments to individual girders was found to be substantially different from the case where a uniform stress distribution is assumed across the section.

4. Steel and concrete stresses produced by dead load and vehicle loads are lower than allowable values for two- and three-lane AASHTO HS 20-44 trucks but slightly exceed the allowable values for one lane of proposed class 2 construction vehicles. However, all observed stresses were well below the proportional limit.

ACKNOWLEDGMENT

This investigation was sponsored by the Business and Transportation Agency, Caltrans, and the Federal Highway Administration, U.S. Department of Transportation. The opinions, findings, and conclusions expressed are ours and not necessarily those of the sponsors.

REFERENCES

1. Standard Specifications for Highway Bridges, 12th ed. AASHTO, Washington, DC, 1977.
2. K.J. Willam and A.C. Scordelis. Cellular Structures of Arbitrary Plan Geometry. Journal of the Structural Division, ASCE, Vol. 98, No. ST7, July 1972.
3. C.D. Comartin and A.C. Scordelis. Analysis and Design of Skew Box Girder Bridges. Univ. of California, Berkeley, Structural Engineering and Structural Mechanic Rept. UC SESM 72-14, Dec. 1972.
4. W.G. Godden and M. Aslam. Model Studies of Skew Multicell Girder Bridges. Journal of the Engineering Mechanics Division, ASCE, Vol. 99, No. EM1, Feb. 1973.
5. M.R. Wallace. Studies of Skewed Concrete Box Girder Bridges. TRB, Transportation Research Record 607, 1976, pp. 50-55.
6. A.C. Scordelis. Analytical Solutions for Box Girder Bridges. Proc., Conference on Modern Developments in Bridge Design and Construction, Cardiff, Great Britain, April 1971.
7. A.C. Scordelis. Analytical and Experimental Studies of Multi-Cell Concrete Box Girder Bridges. Bull., International Association for Shell and Spatial Structures, Madrid, No. 58, Aug. 1975.
8. A.C. Scordelis, J.G. Bouwkamp, and S.T. Wasti. Structural Behavior of a Two Span Reinforced Concrete Box Girder Bridge Model: Vols. 1-3. Univ. of California, Berkeley, Structural Engineering and Structural Mechanics Rept. UC SESM 71-5, 71-6, and 71-7, Oct. 1971.
9. A.C. Scordelis, J.G. Bouwkamp, and S.T. Wasti. Study of AASHO Loadings on a Concrete Box Girder Bridge. HRB, Highway Research Record 428, 1973, pp. 22-31.
10. A.C. Scordelis, J.G. Bouwkamp, and S.T. Wasti. Structural Response of a Concrete Box Girder Bridge. Journal of the Structural Division, ASCE, Vol. 99, No. ST10, Oct. 1973.
11. A.C. Scordelis, J.G. Bouwkamp, and S.T. Wasti. Ultimate Strength of a Concrete Box Girder Bridge. Journal of the Structural Division, ASCE, Vol. 100, No. ST1, Jan. 1974.
12. A.C. Scordelis, J.G. Bouwkamp, and P.K. Larsen. Structural Behavior of a Curved Two Span Reinforced Concrete Box Girder Bridge Model: Vols. 1-3. Univ. of California, Berkeley, Structural Engineering and Structural Mechanics Rept. UC SESM 74-5, 74-6, and 74-7, Sept. 1974.
13. A.C. Scordelis and P.K. Larsen. Structural Response of Curved RC Box Girder Bridge. Journal of the Structural Division, ASCE, Vol. 103, No. ST8, Aug. 1977.
14. A.C. Scordelis, P.K. Larsen, and L.G. Elfgren. Ultimate Strength of Curved RC Box Girder Bridge. Journal of the Structural Division, ASCE, Vol. 103, No. ST8, Aug. 1977.
15. A.C. Scordelis, L.G. Elfgren, and P.K. Larsen. Time Dependent Behavior of Box Girder Bridges. Journal of the American Concrete Institute, Title 76-9, Jan. 1979.
16. A.C. Scordelis, J.G. Bouwkamp, S.T. Wasti, and D. Anicic. Structural Behavior of a Skew Two Span Reinforced Concrete Box Girder Bridge Model: Vols. 1-4. Univ. of California, Berkeley, Structural Engineering and Structural Mechanics Rept. UC SESM 80-1, 80-2, 80-3, and 80-4, June 1980.
17. A.C. Scordelis, S.T. Wasti, and F. Seible. Structural Response of Skew RC Box Girder Bridge. Journal of the Structural Division, ASCE, Vol. 108, No. ST1, Jan. 1982.
18. A.C. Scordelis, J.G. Bouwkamp, S.T. Wasti, and F. Seible. Ultimate Strength of Skew RC Girder Bridge. Journal of the Structural Division, ASCE, Vol. 108, No. ST1, Jan. 1982.
19. A.C. Scordelis and F. Seible. Time-Dependent Behavior of a Skew RC Box Girder Bridge. Journal of the American Concrete Institute, Concrete International (in preparation).

Publication of this paper sponsored by Committee on Concrete Bridges.